NASA Contractor Report 178278

ICASE REPORT NO. 87-24

ICASE

SINGULAR FINITE ELEMENT METHODS

George J. Fix

INSTITUTE FOR COMPUTER APPLICATIONS IN SCIENCE AND ENGINEERING
NASA Langley Research Center, Hampton, Virginia 23665

Operated by the Universities Space Research Association

NASA

National Aeronautics and
Space Administration

Langley Research Center
Hampton, Virginia 23665

SINGULAR FINITE ELEMENT METHODS

George J. Fix

ABSTRACT

Singularities which arise in the solution to elliptic system are often of great technological importance. This is certainly the case in models of fracture of structures. In this report, we survey the way singularities are modeled with special emphasis on the effects due to nonlinearities.

1. INTRODUCTION

The key property of elliptic systems is that their solution tends to be as smooth as the data and other factors permit. This is in striking contrast to hyperbolic systems where singular behavior (e.g., shocks) can arise even if all inputs are smooth.

To illustrate this, consider the following model problem defined in a bounded region Ω of $\mathbb{R}^n$:

$$(1.1) \qquad \text{div}[a\ \text{grad}\phi] = f \qquad \text{in}\ \Omega$$

$$(1.2) \qquad B[\phi] = g \qquad \text{on}\ \partial\Omega.$$

The boundary operator B has the form

$$(1.3) \qquad B[\phi] = \alpha\ \frac{\partial\phi}{\partial\nu} + \beta\phi,$$

where $\underline{\nu}$ is the outer normal to $\partial\Omega$. Thus the inputs to this system are the coefficients a, α, β, the data f, g, and the region Ω. If all of these are smooth, then the same is true of the solution ϕ.

This means that singular behavior can arise only in the cases where the inputs are irregular. The following are examples of technical importance.

<u>Case 1: Irregular Boundaries</u>. The study of fracture and crack propagation involves elliptic systems of various orders depending on the type of problem being modelled [1] - [2]. Torsion problems are second order (like (1.1)), while plates involve fourth order equations, and shell problems are

even of higher order [3] - [4]. Nevertheless, the region Ω in question generally contains a slit as in Figure 1.1 with the point P being the crack tip. In the linear, second order case (a = 1 in (1.1)) it can be shown that with Dirichlet boundary condition (α = 0, β = 1 in (1.2)) the solution ϕ behaves like

$$(1.4) \qquad\qquad \phi = \sigma r^{1/2} \sin(\theta/2) + o(r)$$

near the crack tip ($r \to 0$). Thus the gradient is singular at the crack tip:

$$(1.5) \qquad\qquad |\nabla\phi| = 0(r^{-1/2}) \quad \text{as} \quad r \to 0.$$

The coefficient σ of the singularity is of great technical importance, and is called the stress intensity factor. Knowing it permits estimates on crack behavior via energy release rates [5] - [6].

While singular behavior at corners in solid mechanics is of great technical significance, in fluid mechanics corner singularities are often irrelevant artifacts. For example, linear potential flow over a flat plate involves the same equations and geometry as discussed above [7]. In this case, the gradient $\nabla\phi$ is the velocity field and hence (1.5) predicts a square root singularity at P. This does not occur in real flows and is an artifact of the linearization. A proper nonlinear analysis shows the velocity singularity is a good deal milder. This and other nonlinear effects are discussed in Section 3.
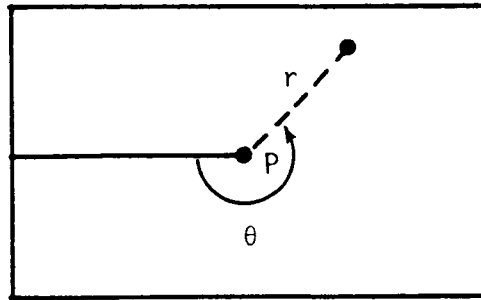
Figure 1.1. The Slit Region Ω: (r,θ) are polar coordinates at   P

Case 2:   Discontinuous Boundary Operators.   Singularities can arise when the boundary conditions (1.2) abruptly change type, or what is the same, when the coefficients α, β in (1.3) are discontinuous.   An example is given in Figure 1.2.   Observe that in this case the Neuman condition

$$\frac{\partial \phi}{\partial \nu} = 0$$

is a symmetry condition, and hence this case is exactly the one represented in Figure 1.1.   In particular, the singularity is described by (1.4).   Most of the applications in fluid and solid mechanics involving discontinuous boundary operators arise in this manner.
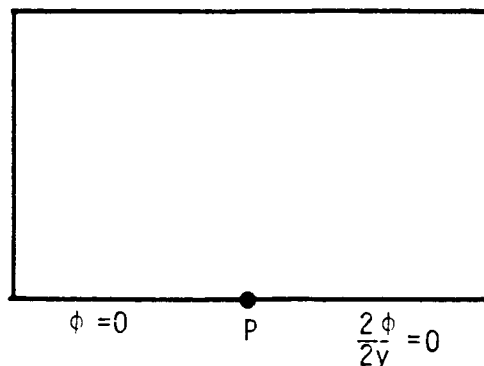

$\phi = 0$ P $\frac{2\phi}{2y} = 0$

Figure 1.2. Discontinuous Boundary Conditions

Case 3:   Discontinuous Coefficients.   Discontinuities in the coef-
ficient   a   in (1.1) can also generate singularities in the solution ϕ.
Cases of technical importance include diffusion problems in regions Ω con-
sisting of different materials [8] - [9].   A typical example is shown in
Figure 1.3.   Using polar coordinates (r,θ) at the point   P, it can be shown
that the singularity behaves like

(1.6) $\phi = \sigma r^\lambda \Phi(\theta)$

plus higher order terms in   r   for a suitable function Φ.   The exponent
depends on the (constant) values a_j of   a   in each of the regions
Ω_j (j = 1,$\cdots$,4).   In general, these singularities can be far more serious
than the square root singularity in (1.4).   In particular, $\lambda > 0$ can be
made arbitrarily small for appropriate choices of $a_1,\ldots,a_4$ [9].
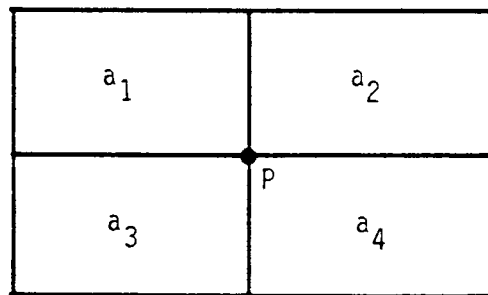

Figure 1.3.   The region Ω for the apriori bound (2.22)

Case 4:   Nonsmooth Data.   Cases where for   g   in (1.1) - (1.2) are not
smooth arise in solid mechanics when bodies are subject to random loads
[10].   To date, these have been best treated using the techniques of stochas-
tic differential equations since singular behavior of the solution ϕ tends

to be distributed over the entire region Ω. These techniques are not treated in this paper, and the reader is referred to [11] for more details.

The presence of singularities, such as described above, tend to significantly affect the rates of convergence for both finite difference as well as finite element schemes [12]. Except for Case 4 cited above, two approaches have been used to treat the singular behavior. One, generally called the singular element method because of the way it is used in finite element schemes, attempts to incorporate the singular behavior into the approximation. The other approach uses grid refinement.

To put this paper into proper perspective, it should be clearly noted that, in general, grid refinement is the best approach. This is particularly the case when adaptive strategies can be incorporated into the approximation [13] – [15]. Singular elements tend to be useful only in very special circumstances, some of which are cited below. However, the methodology used to derive singular elements still remains quite relevant. The point is a priori knowledge of the nature of the singularity can be of practical benefit even if this information is used only indirectly. This is certainly true of grid refinement as well as h, p, and h-p versions of the finite element method [15] – [16]. Because of this, these methodologies will receive the primary emphasis in this paper.

Sections 2 and 3 are devoted to the types of singular behavior that can arise in elliptic systems. Section 3 considers nonlinear effects, and this material is apparently new. The final section concentrates on practical issues associated with singular elements along with selected numerical results.

2. SINGULAR BEHAVIOR IN LINEAR SYSTEMS

For simplicity attention will be confined to problems with corner singularities. Interface problems (Case 3 in Section 1) are treated with similar techniques.

In the linear case the starting point is the construction of explicit solutions using separation of variables for constant coefficient problems and simple geometries. Then using well developed techniques from the theory of partial differential equation (e.g., modifiers and frozen coefficients iterations) one can analyze problems with variable coefficients and rather broad classes of regions Ω ([17] - [18]).

Apparently, the first researcher to realize that the form of singularities can be obtained by a local separation of variables was L. Williams [19]. To describe the results in this classic paper, consider the sectorial region shown in Figure 2.1 letting (r,θ) denote polar coordinates, then (1.1) (with a = 1) becomes

$$(2.1) \qquad \frac{\partial^2 \phi}{\partial r^2} + \frac{1}{r} \frac{\partial \phi}{\partial r} + \frac{1}{r^2} \frac{\partial^2 \phi}{\partial \theta^2} = 0.$$

Assuming a solution of the form

$$(2.2) \qquad \phi = r^\lambda \Phi(\theta),$$

we are led to an eigenvalue problem for the exponent λ and the function Φ:

$$(2.3) \qquad \frac{d^2 \Phi}{d\theta^2} + \lambda^2 \Phi = 0.$$

The type of singularity obtained thus depends on the boundary conditions. Dirichlet conditions

$$(2.4) \qquad \Phi(0) = \Phi(\theta_0) = 0$$

yield

$$(2.5) \qquad r^{\pm \sigma} \sin \sigma \theta, \qquad \sin \sigma \theta_0 = 0.$$

The relevant solution is the one with the smallest positive index σ. This gives

$$(2.6) \qquad \phi = r^{\frac{\pi}{\theta_0}} \sin(\frac{\pi \theta}{\theta_0})$$

as the dominant singular term. Observe that $\nabla \phi$ is finite at the corner point P, if and only if $0 < \theta_0 < \pi$; i.e., reentrant corners $(\theta_0 > \pi)$ yield unbounded gradients. In the case of a crack shown in Figure 1.1, we have $\theta_0 = 2\pi$, and hence (2.6) reduces to the square root singularity given by (1.4).

It is important to note that the order of the differential operator exerts an important influence on the type of singularities that are obtained. For example, consider the fourth order equation

$$(2.7) \qquad \Delta^2 \phi = 0$$

defined in the section shown in Figure 2.1. Assuming a solution of the form

(2.8)
$$\phi = r^{\lambda+1}\Phi(\theta),$$

we obtain

(2.9) $\Phi(\theta) = a_1 \sin(\lambda + 1)\theta + a_2 \cos(\lambda + 1)\theta + b_1 \sin(\lambda - 1)\theta + b_2 \cos(\lambda - 1)\theta.$

The constants a_j, b_j depend on the boundary conditions to be imposed on $\theta = 0$ and $\theta = \theta_0$. For example, along a clamped radial edge one has

(2.10)
$$\omega = 0, \quad \frac{1}{r}\frac{\partial \omega}{\partial \theta} = 0,$$

while a simply supported edge gives

(2.11)
$$\omega = 0, \quad \sigma_\theta = 0,$$

where

(2.12)
$$\sigma_\theta = \frac{1}{r^2}\frac{\partial^2 \omega}{\partial \theta^2} + \frac{1}{r}\frac{\partial \omega}{\partial r} + \nu \frac{\partial^2 \omega}{\partial r^2},$$

ν being the Poisson ratio. Substituting into either of the boundary conditions gives a nonlinear equation for the exponent λ. Except for special cases this equation must be solved numerically, i.e., explicit formulas for the exponents are not known. Nevertheless, a number of qualitative features of solutions to these equations are known (along with specific numerical values in technically important cases [19]).

An important point is that solutions λ can be complex. This implies that oscillatory behavior in the radial directions can occur. This is particularly relevant for cases where the stress intensity factors are approximated using only nodal values of the solution ϕ.

In the case of a crack (Figure 1.2) it can be shown that $\lambda = \frac{1}{2}$. Thus the stress σ_θ given by (2.12), which is the analog of the gradient for the fourth order case, displays a square root singularity.
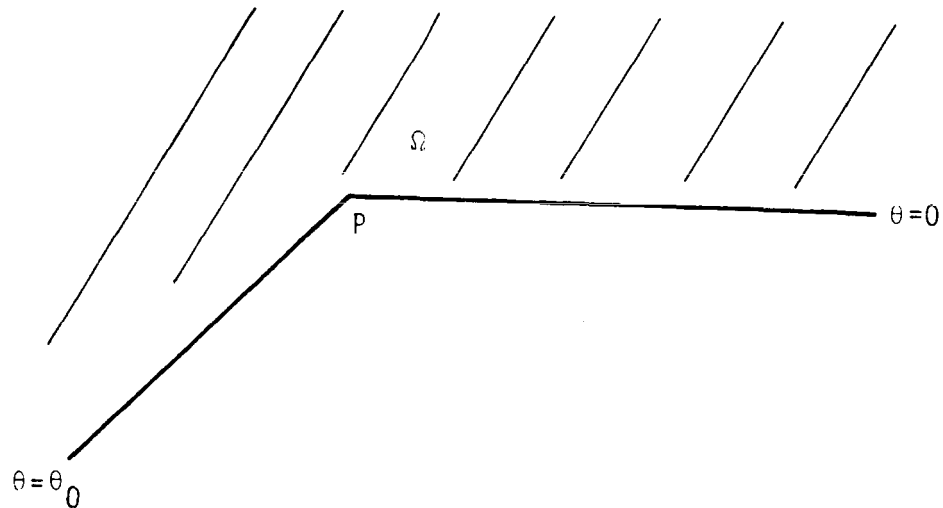

Figure 2.1. The sector Ω

Another issue of technical importance concerns the effect of dimension. The direct generalization of William's work to three dimensions involves the conical region shown in Figure 2.2. Letting (r,θ,ψ) denote spherical coordinates, one seeks a solution of the form

$$(2.13) \qquad \phi = r^\lambda \Phi(\theta,\psi).$$

In the second order case, one is again lead to an eigenvalue problem except now for the Laplace-Beltrami operator on the boundary surface of Ω:

$$(2.14) \qquad \frac{1}{\sin^2\theta} \frac{\partial^2\Phi}{\partial\psi^2} + \frac{1}{\sin\theta} \frac{\partial}{\partial\theta} (\sin\theta\frac{\partial\Phi}{\partial\theta}) + \lambda(\lambda + 1)\Phi = 0.$$

A further separation of variables gives

$$(2.15) \qquad \Phi(\theta,\psi) = \sin(m\psi + \alpha)P(\theta),$$

where P satisfies the Legendre equation

$$(2.16) \qquad \frac{d}{d\mu} [(1 - \mu^2) \frac{dP}{d\mu}] + [\lambda(\lambda + 1) - \frac{m^2}{1 - \mu^2}]P = 0$$

with $\mu = \cos\theta$. In the case of Dirichlet boundary conditions, solutions are obtained by requiring

$$(2.17) \qquad P(\mu_0) = 0, \qquad \mu_0 = \cos\theta_0.$$

Properties of these solutions have been studied for the case $0 < \theta_0 < \pi$ [20]. The dominant singularity is independent of ψ (i.e., $m = 0$, $\alpha = \frac{\pi}{2}$ in (2.15)). In this case (2.16) can be solved with Legendre functions $P = P_\lambda$ and (2.17) reduces to a nonlinear equation for λ. Many of the characteristics of the two dimensional case reappear here. For example, $|\nabla\phi|$ is finite at P only in the case of convex region $(0 < \theta_0 < \frac{\pi}{2})$.

Interestingly, this analysis runs into trouble in the case of a crack $\theta_0 = \pi$.[(*)] Here, (2.17) does not have solutions with $m = 0$ since the only solutions to (2.16) with $m = 0$ which are finite on $-1 \leq \mu \leq 1$ are Legendre polynomials $P_n(\lambda = n)$ which satisfy $|P_n(\pm 1)| = 1$. The net result is the question of the completeness of the functions in which the singular behavior is described. Nevertheless, if one were to accept the limiting behavior as $\theta \to \pi$ as valid, then the apparently ubiquitous square root singularity reemerges.
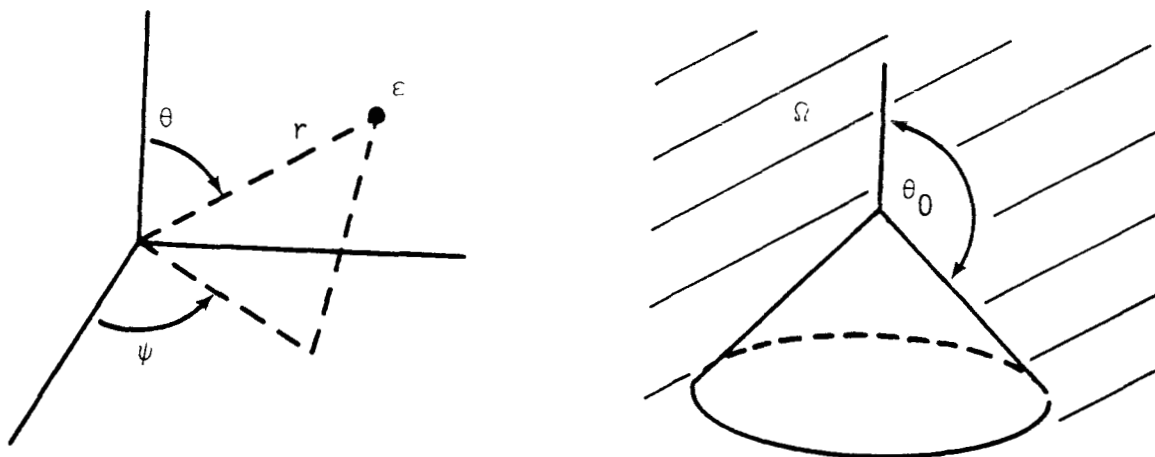

Figure 2.2. Spherical coordinates and the conical region Ω.

The open question of completeness of the functions used to describe singular behavior in three dimensions is also present in regions other than cones. Thus a rigorous account of how solutions behave near planar slices in Ω, a case of considerable technical importance is still not completely known.

Elementary solutions such as those described above can be used to obtain results for rather general regions Ω and for problems with variable coefficients. Typically this approach will not yield explicit behavior, but rather shows that the solutions lie in appropriate Sobolev spaces. With most grid refinement techniques, this information is almost as useful as knowing the explicit behavior.

To fix ideas, consider the second order case (1.1) - (1.2), where a is a smooth function of the spatial variables and $\alpha = 0$, $\beta = 1$ (Dirichlet boundary conditions). Let Ω be the region shown in Figur 2.3 which has a corner at P but is otherwise smooth. Note that the edges leading to P do not necessarily have to be straight. For this region we introduce the following weighted Sobolev spaces in terms of the radial distance r to P. Indeed, let

$$(2.18) \qquad \|\omega\|_{0,\beta} = \{\int_{\Omega} r^{\beta} |\omega|^2\}^{1/2}$$

be a weighted L_2 for the given exponent $\beta \in \mathbb{R}$. The higher order spaces involve derivatives. Thus

$$(2.19) \qquad \|\omega\|_{1,\beta} = \{\int_{\Omega} r^{\beta} [|\nabla\omega|^2 + \omega^2]\}^{1/2}$$

with analogous definitions for $\|\omega\|_{t,\beta}$ $(t > 1)$. A priori bounds on the solution ϕ were first obtained in a fundamental paper by Kondrat´ev [17] (see also [18]). A typical result in the case of homogeneous boundary conditions ($g = 0$ in (1.2)) shows that if

$$(2.20) \qquad t + 1 - (\pi/\theta_0) < \beta \leq t + 1$$

and

$$(2.21) \qquad \|f\|_{t,\beta} < \infty,$$

then there is a constant $0 < C < \infty$, depending only on t, β, Ω, and a, for which

$$(2.22) \qquad \|\phi\|_{t+2,\beta} \leq C\|f\|_{t,\beta}.$$

The analysis requires that Ω satisfy an exterior cone condition and hence the interior angle θ_0 is restricted to $0 < \theta_0 < 2\pi$. This inequality can be verified directly in the cases where the explicit singular behavior is known.
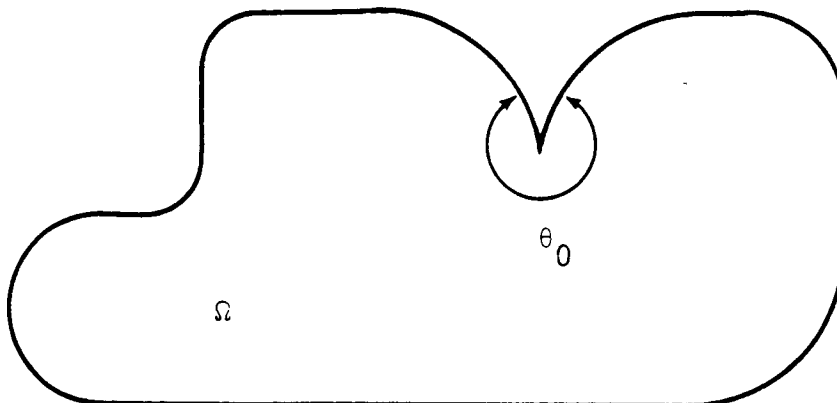

Figure 2.3

The practical use of a priori bounds like (2.22), and well as use of the explicit singular behavior (when known) will be discussed in the last section.

3. SINGULAR BEHAVIOR IN NONLINEAR SYSTEMS

In this section, we shall study the effects of nonlinearities on singular behavior. In this setting, the basic paradigm underlying the analysis in the linear case, namely separation of variables, is not available, hence different techniques are needed.

To fix ideas, we consider (1.1) with Dirichlet boundary conditions ($\alpha = 0$, $\beta = 1$) in the sector shown in Figure 2.1. We assume the coefficient depends on the gradient $\nabla\phi$ as

$$(3.1) \qquad a = a(|\nabla\phi|^2).$$

For the problem to be elliptic, we need

$$(3.2) \qquad \frac{d}{dt}[a(t)^2 t] > 0$$

uniformly throughout Ω.

An early approach to this problem was given by Tolksdorf [21]. He looked for solutions of the form

$$(3.3) \qquad \phi = r^\lambda \Phi(\theta),$$

and showed that λ, Φ are related through a nonlinear eigenvalue problem.

A key parameter in the latter is the number

$$(3.4) \qquad q = \lim_{t \to \infty} [t \, \frac{da(t)}{dt}/a(t)].$$

As will be seen below, this number determines the nonlinear effects on the singularity. Observe that $q = 0$ in the linear case, and for this system to be elliptic it is necessary that

$$(3.5) \qquad q > -\frac{1}{2}.$$

Because of the nonlinearities, it is not possible to get explicit solutions to the nonlinear eigenvalue problem. However, using maximum principle arguments with comparison functions, Tolksdorf was able to obtain the following bounds on the minimal exponent λ in (3.3):

$$(3.6) \qquad \lambda_1(\theta_0) \leq \lambda \leq \lambda_2(\theta),$$

where

$$(3.7) \qquad \lambda_1(\theta) = \frac{q\alpha_0 + \sqrt{(2q + 1)(4q + 1) + q^2\alpha_0^2}}{\alpha_0(4q + 1)}$$

and

$$(3.8) \qquad \lambda_2(\theta) = \frac{q\alpha_0 + \sqrt{(2q + 1) + q^2\alpha_0^2}}{\alpha_0(2q + 1)}$$

with $\theta_0 = \alpha_0\pi$.

Unfortunately, as will be shown below, the inequalities in (3.6) are not strict except in the linear case $q = 0$. Nevertheless, the results do contain useful information. For example, $0 < \lambda < 1$ for reentrant corners $(\pi < \theta_0 < 2\pi)$, and hence $|\nabla\phi|$ is singular in these cases. Moreover, this is the only property that survives from the linear case, and the nonlinear terms definitely affect the asymptotic behavior as $r \to 0$. It is also noteworthy that this approach can also be used in three and higher dimensions.

Sharp results can be obtained for the case of two dimensions. The starting point is a fundamental paper by L. Lehman [22]. This work was limited to the linear case, however, the function theoretic approach used did not require the explicit construction of solutions via separation of variables. The exact form of the singularity was obtained, but in an indirect manner using appropriate transformations and analytic continuation. This is why the results are limited to planar regions; however, they do point the way to an approach for the nonlinear case via a hodograph transformation.

In particular, we let u,v denote the components of the gradient $\nabla\phi$ and rewrite (1.1) as

$$(3.9) \qquad (a + a^\nabla u^2) \frac{\partial u}{\partial x} + (2a^\nabla uv) \frac{\partial u}{\partial y} + (2a^\nabla uv) \frac{\partial v}{\partial x} + (a + a^\nabla v^2) \frac{\partial v}{\partial y} = 0$$

$$(3.10) \qquad \frac{\partial u}{\partial y} - \frac{\partial v}{\partial x} = 0,$$

where $a^\nabla = \frac{da}{dt}$. The hodograph transformation takes the form

$$(3.11) \qquad x = x(u,v), \quad y = y(u,v).$$

At points where the Jacobian of the transformation

(3.12)
$$J = \frac{\partial u}{\partial x} \frac{\partial v}{\partial y} - \frac{\partial u}{\partial y} \frac{\partial v}{\partial x} = \frac{\partial^2 \phi}{\partial x^2} \frac{\partial^2 \phi}{\partial y^2} - \frac{\partial^2 \phi}{\partial x \partial y}$$

is nonzero, we have

(3.13)
$$(a + 2a^\nabla u^2) \frac{\partial y}{\partial v} - (2a^\nabla uv - (2a^\nabla uv) \frac{\partial y}{\partial u} + (a + 2a^\nabla v^2) \frac{\partial x}{\partial t} = 0$$

(3.14)
$$\frac{\partial x}{\partial v} - \frac{\partial y}{\partial u} = 0.$$

Because the last relation, a potential ψ can be introduced so that

(3.15)
$$\frac{\partial \psi}{\partial u} = x, \qquad \frac{\partial \psi}{\partial v} = y.$$

This gives

(3.16)
$$(a + 2a^\nabla u^2) \frac{\partial^2 \psi}{\partial v^2} - 4a^\nabla uv \frac{\partial^2 \psi}{\partial u \partial v} + (a + 2a^\nabla v^2) \frac{\partial^2 \psi}{\partial u^2} = 0.$$

Thus the hodograph takes the original nonlinear problem into a linear one. Observe that ellipticity of the equation is not affected by the transformation.

Hodograph transformations have been used in a number of problems [7]. The technical difficulty has typically been in deriving boundary conditions in the hodograph plane. In fact, the traditional approach in fluid dynamics is to let the boundary conditions so obtained actually define the problem that is being solved [7, Ch. XX]. Here no such problems arise, as can be anticipated

from a careful study of Lehman's work. The cases of a reentrant $(\theta_0 > \pi)$ or convex $(\theta_0 < \pi)$ corner are different, so for brevity we consider only the former since it is the most important.

The boundary transformations under the hodograph are given in Figure 3.1. In particular, the sector $\Omega: 0 \le \theta \le \theta_0$ gets mapped into a double cone $\hat{\Omega}$ with angle $\theta_0 - \pi$.
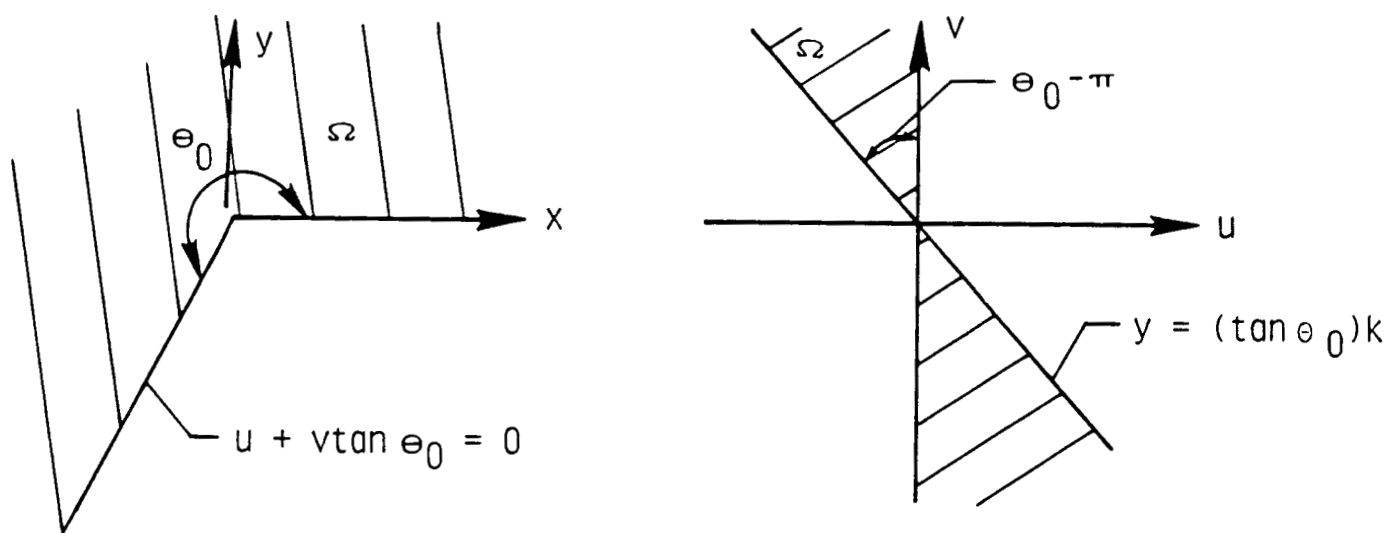
Figure 3.1. The hodograph

Introducing polar coordinates

(3.17)
$$u = \rho\cos\omega, \qquad v = \rho\sin\omega.$$

It can be shown that (3.16) reduces to

(3.18)
$$\left(\frac{a}{a + 2a^\nabla\rho 2}\right)\frac{\partial^2\psi}{\partial P_2} + \frac{1}{\rho}\frac{\partial\psi}{\partial\rho} + \frac{1}{\rho^2}\frac{\partial^2\psi}{\partial\omega^2} = 0.$$

Moreover, Dirichlet boundary conditions $\psi = 0$ on $\partial\hat{\Omega}$ can be used.

Tolksdorf's work shows that $\nabla\phi$ is singular at the corner point $r = 0$. Thus in the hodograph plane it is the behavior at $\rho = \infty$ which is relevant. Since the coefficient in (3.18) is smooth, Kondret'ev's work [17] shows one can freeze it in the neighbor of the singularity; i.e., replace it with

$$(3.19) \qquad \lim_{t \to \infty} \left(\frac{a}{a + 2a\nabla_\rho^2}\right) = \frac{1}{1 + 2q} \, ,$$

where q is the index (3.4) appearing in Tolksdorf's work. The resulting problem

$$(3.20) \qquad \left(\frac{1}{1 + 2q}\right) \frac{\partial^2\psi}{\partial\rho^2} + \frac{1}{\rho}\frac{\partial\psi}{\partial\rho} + \frac{\partial^2\psi}{\partial\theta^2} = 0$$

can now be solved by separation of variables. In particular, letting

$$(3.21) \qquad \psi = \rho^\sigma \sin\left(\frac{\omega\pi}{\theta_0 - \pi}\right)$$

we obtain

$$(3.22) \qquad \sigma = \pm\sigma_0, \qquad \sigma_0 = q + \sqrt{q^2 + \frac{2q + 1}{(\alpha_0 - 1)^2}} \, ,$$

where $\theta_0 = \alpha_0\pi$. Since it is the behavior at ∞ which is relevant, we take $\sigma = -\sigma_0$. Expressing the results in terms of the radial coordinate r in the physical plane, we have

$$(3.23) \qquad |\nabla\psi| \sim r.$$

Hence

(3.24)
$$\nabla\phi \sim r^{\sigma_0/(\sigma_0 + 1) - 1} ,$$

or what is the same the exact exponent λ in (3.3) is given by

(3.25)
$$\lambda = \frac{\sigma_0}{1 + \sigma_0} , \qquad \sigma_0 = q^2 + \sqrt{q^2 + \frac{2q + 1}{(\alpha_0 - 1)^2}} .$$

Observe that in terms of the lower bound λ_1 and upper bound λ_2 cited above we have

(3.26)
$$\lambda_1 < \lambda < \lambda_2$$

except in the linear case (q = 0) where

$$\lambda_1 = \lambda = \lambda_2 = \frac{1}{\alpha_0} .$$

Consider now the case of a slit where $\alpha_0 = 2$. The exponent λ reduces to

(3.26)
$$\lambda = \frac{2q + 1}{2q + 2} .$$

Observe that if q is negative, then

(3.27)
$$\lambda < \frac{1}{2} ,$$

i.e., the singularity is stronger than that occurring in the associated linear problem. The limiting case is $q = -\frac{1}{2}$, and the problem is no longer elliptic for smaller values of q. That this type of analysis fails is to be anticipated. Indeed, the equations will be hyperbolic in such cases, and the presence of real charcteristics means that the type of singularity obtained depends on information in the far field away from the singular point.

If, on the other hand, q > 0 we have a situation where the nonlinear terms smooth the singularity; i.e.,

(3.28) $$\lambda > \frac{1}{2} .$$

A case of interest is compressible potential flow [7] where

(3.29) $$a(t)^{\delta-1} = M_\infty^2 [C_0^2 - (\frac{\delta - 1}{2})t].$$

It is readily seen that

(3.30) $$q = \frac{1}{\delta - 1}$$

in this case, and so

(3.31) $$\lambda = \frac{1 + \delta}{2\delta} .$$

For dry air $\delta = 1.405$ and λ is approximately .9. As far as numerical approximations are concerned, this is a far less serious singularity than $\lambda = .5$ predicted for linear flows.

4. PRACTICAL CONSIDERATIONS

To fix ideas, consider the planar region shown in Figure 2.3, and the linear second order case.

As far as (nonadaptive) mesh refinement is concerned, the starting point is the identification of a region Ω_s about the singular point where mesh refinement is used. An important practical consideration is that with local mesh refinement the number of points used in Ω_s need only grow like $O(|\ln h|^2)$, where h is the far field mesh spacing. The key to this is the existence of an a priori bound like (2.22). For simplicity, we take the case $t = 0$ so

$$(4.1) \qquad 1 - \pi/\theta_0 < \beta < 1.$$

The grid goes as follows. For triangles adjacent to P the diameter δ, satisfies

$$(4.2) \qquad \delta \leq (\text{constant}) h^{\frac{1}{1 - \beta}}.$$

This is increased by a constant factor until the far field uniform grid with spacing h is obtained. Grids of this type have been used in [23] for standard finite element methods and in [4] for those based on least square approximations.

It can be shown that for such grids the approximation ϕ_n using linear elements satisfies

$$(4.3) \qquad \left\{ \int |\nabla(\phi - \phi_n)|^2 \right\}^{1/2} \leq C\, h\, \left\{ \int r^{2\beta} |D^2 \phi| \right\}^{1/2}.$$

Numerical evidence shows that if approximate difference quotients are used, then approximations σ_h to the stress intensity factor σ can be obtained satisfying

$$(4.4) \qquad\qquad \sigma - \sigma_h = 0(h^{3/2})$$

in the case of a slit region (Figure 1.1) [25]. It is a point of practical significance that the form of the singularity must be known in order to establish the relevant difference approximation for σ_n. Path independent J-integrals [26] can be used as an alternative, however, they produce approximations which converge at lower rates, typically $0(h)$ when using linear elements.

In a singular element approach, one seeks approximations in the form

$$(4.5) \qquad\qquad \phi_h = \sigma_h \phi_s + \sum_j \phi_j N_j,$$

where ϕ_s is the (known) singular function, σ_h is the intensity of the singularity (to be computed), and N_j are the piecewise linear nodal functions. Since variational methods typically yield best approximations (in suitable norms), the term $\sigma_h \phi_s$ in effect substracts out the singularity; i.e., for a suitable number σ (the exact intensity)

$$(4.6) \qquad\qquad \|\phi - \sigma\phi_s\|_{2,0} < \infty,$$

and thus $\cdot \phi - \sigma\phi_s$ can be approximated by piecewise linear functions on a regular grid. Stated differently

(4.7)
$$\inf_{\xi_i, \eta} \| \phi - \eta \phi_s - \sum \xi_i N_i \|_{1,0} \leq Ch \| \phi - \eta \phi_s \|_{2,0}.$$

This means the ϕ_h computed by a finite element approximation will satisfy

(4.8)
$$\| \phi - \phi_h \|_{1,0} \leq Ch.$$

In addition, the intensity σ_h in (4.5) has been observed to converge at the rate found in (4.4) [25].

Substitution of (4.5) into a variational principle typically leads to a matrix problem of the form

(4.9)
$$\begin{bmatrix} K_{11} & K_{1s} \\ K_{s1} & K_{ss} \end{bmatrix} \begin{bmatrix} \underline{\phi} \\ \sigma_h \end{bmatrix} = \begin{bmatrix} \underline{f} \\ f_s \end{bmatrix}$$

where K_{11} is a regular finite element matrix, K_{1s} contains inner products of N_j with ϕ_s, while the number K_{ss} is the inner product of ϕ_s with itself. Note that K_{s1} is 1 x N where N is the number of N_j whose support intersects the support of ϕ_s. For the above error estimates to be uniformly valid as $h \to 0$, it is necessary that the support of ϕ_s be fixed independent of h. Thus N grows like $O(h^{-2})$ as $h \to 0$.

One of the early fears about the use of singular functions was that one might be giving up stability in order to gain greater accuracy. While it is true than the coefficient matrix in (4.9) has a far larger condition number that the standard stiffness matrix K_{11}, this has not created problems in practice [25]. For example, in direct elimination the problems are isolated

in a one dimensional subspace. Indeed, the matrix in (4.9) admits the factorization

$$(4.10) \qquad \begin{bmatrix} K_{11} & K_{1s} \\ K_{s1} & K_{ss} \end{bmatrix} = \begin{bmatrix} L_{11} & \\ L_{s1} & L_{ss} \end{bmatrix} \begin{bmatrix} V_{11} & V_{1s} \\ & V_{ss} \end{bmatrix}$$

where

$$(4.11) \qquad K_{11} = L_{11} V_{11}$$

$$(4.12) \qquad K_{1s} = L_{11} V_{1s}, \qquad K_{s1} = L_{s1} V_{11}$$

$$(4.13) \qquad K_{ss} - L_{s1} V_{1s} = L_{ss} V_{ss}.$$

Thus the bulk of the computation is in the factorization of the standard stiffness matrix K_{11} in (4.11). The bordered parts L_{s1}, V_{s1} are obtained through the (stable) backsolves (4.12), and the only part of the calculation where the instability occurs in the 1×1 problem (4.13) (here $L_{ss} = 1$ and V_{ss}, $K_{ss} - L_{s1} V_{1s}$ are numbers).

Also, note that if the stress intensity factor σ_h is the only quantity of interest, and this is frequently the case, then half of the backsolves can be omitted. Indeed, to get σ_h from (4.9) one backsolves

$$(4.14) \qquad L_{11} \underline{y} = \underline{f} , \qquad L_{ss} \omega = f_s - L_{s1} \underline{y}$$

for $\underline{y}$ and ω. Then

(4.15)
$$V_{ss}\sigma = \omega.$$

The remaining backsolves, i.e.,

(4.16)
$$V_{11}\underline{\phi} = \underline{y} - V_{1s}\sigma,$$

can be omitted.

The rates of convergence for ϕ_h and σ_h are the same as that observed for the case of grid refinement [12]. Thus asymptotically as $h \to 0$ there is not a great deal of difference between the two approaches. Although, as noted earlier, the superiority of grid refinement emerges as adaptivity is incorporated into the approximation.

In practical terms, the singular function approach has the advantage of fewer backsolves (in the case where only the intensity is desired), but suffers the disadvantage of requiring that not only inner products of nodal functions N_j be evaluated, but also inner products of the more complicated singular functions ϕ_s. Both of these effects contribute to the lower order terms in the overall work effect--considered as a function of $\frac{1}{h}$ -- and thus both effects are negligible in the limit as $h \to 0$.

On the other hand, for modest accuracy requirements (h not small) the savings in backsolves tends to be a significant effect. It is exactly in these cases where singular element methods have proven to be useful. To cite a specific numerical example, consider the problem described in Figure 4.1. This problem has been used as a test problem for a large number of different

numerical methods ([25] - [30]), and it is known that the stress intensity factor is

$$\sigma = .1917$$

(to the number of decimals shown). Using a single singular function on a uniform grid with $h = \frac{1}{8}$ (65 unknowns) gives

$$\sigma_h = .1862$$

while a β-grid refinement with 16 unknowns (and over three times the CPU cycles and storage requirements) gave

$$\sigma_h = .1621$$

with finer grids; however, the differences in overall work for a given accuracy rapidly disappears [27].

Another special case where singular elements have proven useful is what could be called an "h-p version" of the singular element method. Here one uses more singular functions than would be actually needed, not only to substract out the singularity but also to approximate. For example, in the problem cited above, the use of 8 singular functions and a uniform grid with $h = \frac{1}{4}$ gives

$$\sigma_h = .1916$$

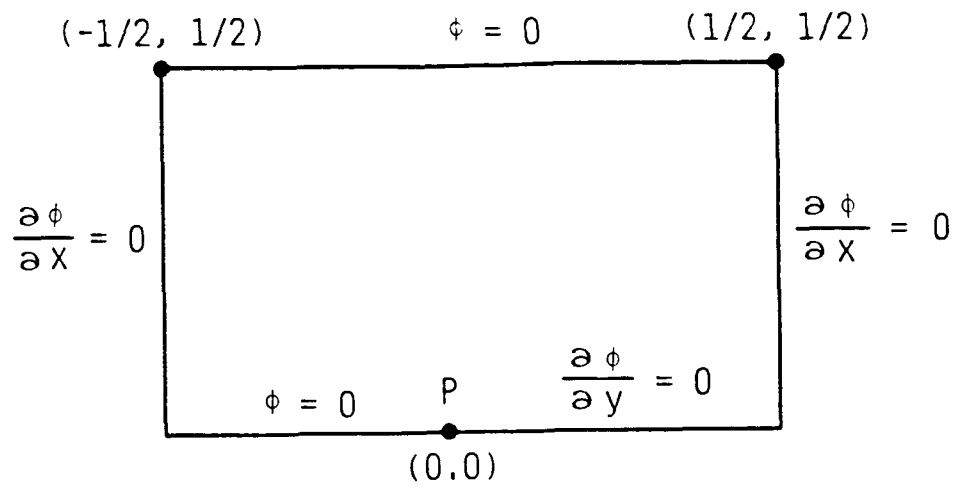(see [27] for this and other examples).

$(-1/2, 1/2)$ $\phi = 0$ $(1/2, 1/2)$

$\dfrac{\partial \phi}{\partial X} = 0$ $\dfrac{\partial \phi}{\partial X} = 0$

$\phi = 0$ P $\dfrac{\partial \phi}{\partial y} = 0$

$(0,0)$

Figure 4.1. Test Problem

REFERENCES

[1]   Swedlow, J. L. (ed.), The Surface Crack, ASME, November, 1972.

[2]   Irwin, G. R., Fracture Mechanics, Pergamon Press, 1960.

[3]   Muskhelishvili, N. I., Some Problems of the Mathematical Theory of Elasticity, Groningen, Holland, 1953.

[4]   Love, A. E. H., The Mathematical Theory of Elasticity, Cambridge, 1927.

[5]   Griffith, A. A., "The phenomenon of rapture and flow in solids," Philos. Trans. Roy. Soc. Ser. (A), Vol. 221, 1920.

[6]   Irwin, G. R., "Analysis of stresses and strains near the end of a crack," J. Appl. Mech., Vol. 24, 1957.

[7]   Milne-Thomson, Theoretical Hydrodynamics, MacMillan, 1968.

[8]   Birkhoff, G., "Numerical Solution of Elliptic Equations," SIAM Publications, 1971.

[9]   Babuska, I., Kellogg, B., The Mathematical Foundation of the Finite Element Method, Edited by A. K. Aziz, Academic Press, 1972.

[10] Schuss, Z., _Theory and Applications of Stochastic Differential Equations_, Wiley, 1980.

[11] Zeman, J. L., _Approximate Analysis of Schochastic Processes in Mechanics_, Springer-Verlag, 1971.

[12] Strang, G., Fix, G. J., _An Analysis of the Finite Element Method_, Academic Press, 1973.

[13] Thompson, J. F., Warsi, ZUA, Mastin, C. W., _Numerical Grid Generation_, North-Holland, 1985.

[14] Miller, K., Miller, N., "Moving finite elements," _SIAM J. Numer. Anal._, Vol. 18, p. 1019, 1981.

[15] Babuska, I., Rheinboldt, W., "Error estimates for adaptive finite element computations," _SIAM J. Numer. Anal._, Vol. 15, 1978.

[16] Babuska, I., Gus, G., "The h-p version of the finite element method," Tech. Note BN-1043, Inst. for Phy. Sci. & Tech., University of Maryland, College Park, 1985.

[17] Kondrat'ev, V. A., "Boundary value problems for elliptic equations in domains with conic or angular points," _Trans. Moscow Math. Soc._, pp. 227-313, 1967.

[18] Kondrat´ev, V. A., Oleinik, O. A., "Boundary value problems for partial differential equations in nonsmooth domains," Russian Math. Surveys, 38:2, pp. 1-86, (1983).

[19] Williams, L., "Stress singularities resulting from various boundary conditions in angular corners," J. Appl. Mech., Vol. 19, pp. 526-528, 1952.

[20] Grisvard, P., Elliptic Problems in Nonsmooth Domains, Boston, Pitman, 1985.

[21] Tolksdorf, P., "On the behavior near the boundary of solutions of quasilinear equations," preprint No. 459, Universität Bonn, 1981.

[22] Lehman, L., "Developments at an analytic corner of solutions of elliptic partial differential equations," J. Math. Mech., Vol. 8, pp. 727-760, 1959.

[23] Babuska, I., Kellogg, R. B., and Pitkäranta, "Direct and inverse error estimates for finite elements with mesh refinements," Numer. Math., Vol. 33, pp. 447-471, 1979.

[24] Cox, C. L., Fix, G. J., "On the accuracy of least square methods in the presence of corner singularities," Comput. Math. Appl., Vol. 10, pp. 463-475, 1984.

[25] Fix, G. J., Gulati, S., Wakoff, G. I., "On the use of singular functions with finite element approximations," *J. Comput. Phys.*, Vol. 13, pp. 209-228, 1973.

[26] Lee, Y., "Shear bands in elastic-perfectly plastic materials," Ph.D. thesis, Carnegie-Mellon University, 1981.

[27] Wakoff, G. I., "Piecewise polynomial spaces and the Ritz-Galerkin Method," Ph.D. thesis, Harvard University, 1970.

[28] Wait, R., Mitchell, A. R., "Corner singularities in elliptic problems," *J. Comput. Phys.*, Vol. 8, pp. 45-52, 1971.

[29] Byskov, E., "Calculation of stress intensity factors using finite element methods," *Internat. J. Fracture*, Vol. 6, pp. 159-168, 1976.

[30] Blackburn, W. S., "Calculation of stress intensity factors at crack tips using special finite elements," *Math. of Finite Elements and Appl.*, J. R. Whiteman, ed., Academic Press, London, 1973.

[31] Blum, H., Dobrowolski, M., "On finite element methods for elliptic equations on domains with corners," *Computing*, Vol. 25, pp. 53-63, 1983.

1. Report No. NASA CR-178278 ICASE Report No. 87-24	2. Government Accession No.	3. Recipient's Catalog No.
4. Title and Subtitle SINGULAR FINITE ELEMENT METHODS		5. Report Date April 1987
		6. Performing Organization Code
7. Author(s) George J. Fix		8. Performing Organization Report No. 87-24
9. Performing Organization Name and Address Institute for Computer Applications in Science and Engineering Mail Stop 132C, NASA Langley Research Center Hampton, VA 23665-5225		10. Work Unit No.
		11. Contract or Grant No. NAS1-18107
12. Sponsoring Agency Name and Address National Aeronautics and Space Administration Washington, D.C. 20546		13. Type of Report and Period Covered Contractor Report
		14. Sponsoring Agency Code 505-90-21-01

15. Supplementary Notes

16. Abstract

Singularities which arise in the solution to elliptic systems are often of great technological importance. This is certainly the case in models of fracture of structures. In this report, we survey the way singularities are modeled with special emphasis on the effects due to nonlinearities.

17. Key Words (Suggested by Authors(s)) singularities, cracks, finite element methods	18. Distribution Statement 02 – Aerodynamics 64 – Numerical Analysis Unclassified – unlimited

19. Security Classif.(of this report) Unclassified	20. Security Classif.(of this page) Unclassified	21. No. of Pages 34	22. Price A03